6. King MJ, Badea I, Solomon J, Kumar P, Gaspar KJ, Foldvari M. Transdermal Delivery of Insulin from a Novel Biphasic Lipid System in Diabetic Rats. Diabetes Technol Ther 2002;4: 479-488.

7. Miyazaki S, Takahashi T, Kubo W, Bachynsky J, Lobenberg R. Poly n-butylcyanoacrylate (PNBCA) nanocapsules as a carrier for NSAIDs: in vitro release and in vivo skin penetration. J Pharm Pharmaceut Sci 2003;6:240-245.

8. Yamaguchi Y, Nagasawa T, Nakamura T, Takenaga M, Mizoguchi M, Kawai S, Mizushima Y, Igarashi R. Successful treatment of photo-damaged skin of nano-scale atRA particles using a novel transdermal delivery. 2005;104:29-40.

9. Ueno Y, Futagawa H, Takagi Y, Ueno A, Mizashima Y. Drug-incorporating calcium carbonate nanoparticles for a new delivery system. J Controlled Release 2005;103:93-98.

10. Yanagawa A, Kudo T, Mizushima Y. A novel particle carrier for transnasal peptide absorption. Jpn J Clin Pharmacol Ther 1995;26:127-128.

11. Jalon EG, Blanco-Prieto MJ, Ygartua P, Santoyo S. PLGA microparticles: possible vehicles for topical drug delivery. Int J Pharm 2001;226:181-184.

12. Haruta S, Hanafusa T, Fukase H, Miyajima H, Oki T. An Effective Absorption Behavior of Insulin for Diabetic Treatment Following Intranasal Delivery Using Porous Spherical Calcium Carbonate in Monkeys and Healthy Human Volunteers. Diabetes Technology& Therapeutics 2003;5:1-9.

13. Ogiso T, Nishioka S, Iwaki M. Dissociation of Insulin Oligomers and Enhancement of Percutaneous Absorption of Insulin. Biol Pharm Bull 1996;19:1049-1054.

14. Koyama Y, Bando H, Yamashita F, Takakura Y, Sezaki H, Hashida M. Comparative Analysis of Percutaneous Absorption Enhancement by d-Limonene and Oleic Acid Based on a Skin Diffusion Model. Pharm Res 1994;11:377-383.

15. Guo J, Ping Q, Zhang L. Transdermal Delivery of Insulin in Mice by Using Lecithin Vesicles as a Carrier. Drug Delivery

2000;7:113-116.

Figure Legends

Figure1. The concentration profiles of serum insulin in ddY mice. Transdermal nanoinsulin (200 μg) was applied trandermally and monomer insulin (3 μg) was administered subcutaneously to ddY mice (n=3, each) as described in Materials and Methods. AUC-I with nanoinsulin and sc monomer insulin was 265 and 431 μIU・hr/ml, respectively, and relative BA is 0.9%.

Figure 2. Time course profiles of blood glucose in ddY mice. Blood glucose levels with transdermal nanoinsulin (200, 100, 50 μg, and 0) and sc monomer insulin (3 μg) was measured as described in Materials and Methods. AUC was 179, 130, and 95 μIU・hr/ml , respectively with 200, 100, and 50 μg of transdermal nanoinsulin, whereas 133 μIU・hr/ml with sc monomer insulin. Relative BA of 200, 100, and 50 μg nanoinsulin was 2.0, 2.9, and 4.3 %, respectively.

*P<0.05, **P< 0.01, ***P<0.001

Table 1 Effects of insulin on blood glucose (Mouse)

	Route (formulation)	n	Dose (μg/head)	$AUC_{0\text{-}6h}$ (U)	Relative $BA_{0\text{-}6h}$ (%)	Glucose nadir level (%)	Glucose at t=0 (mg/dl)
ddY	Dermal (nanoinsulin)	7	200	179	2.0	48.3±3.9	133.9
	sc (monomer)	5	3	133	—	64.1±1.0	
dB/dB	Dermal (nanoinsulin)	5	200	115	1.8	32.5±9.8	414.3
	sc (monomer)	5	5	156	—	57.9±3.4	
kkAy	Dermal (nanoinsulin)	7	200	100	3.4	26.2±7.6	584.0
	sc (monomer)	5	5	74	—	24.1±6.7	

Results are expressed as mean ±SD

Fig. 1

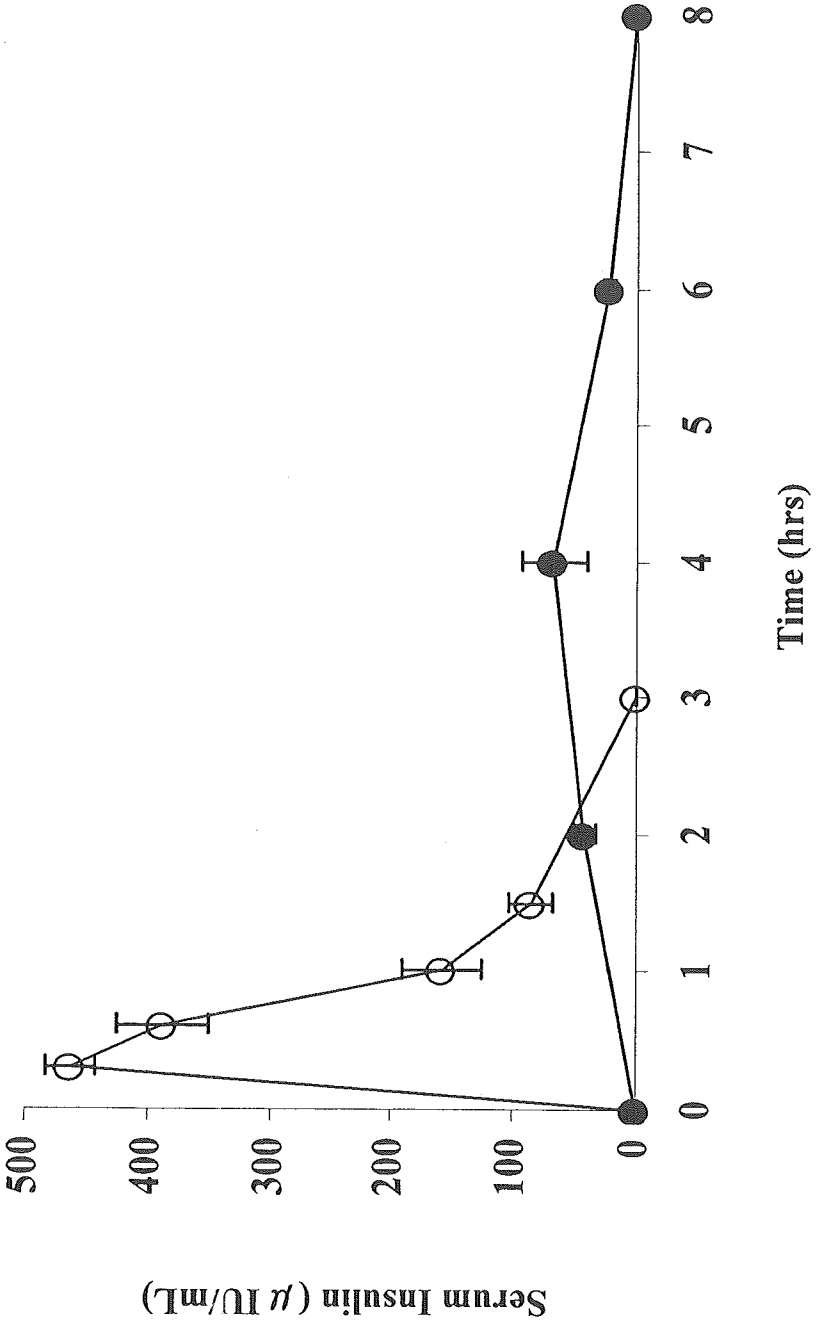

Fig.2

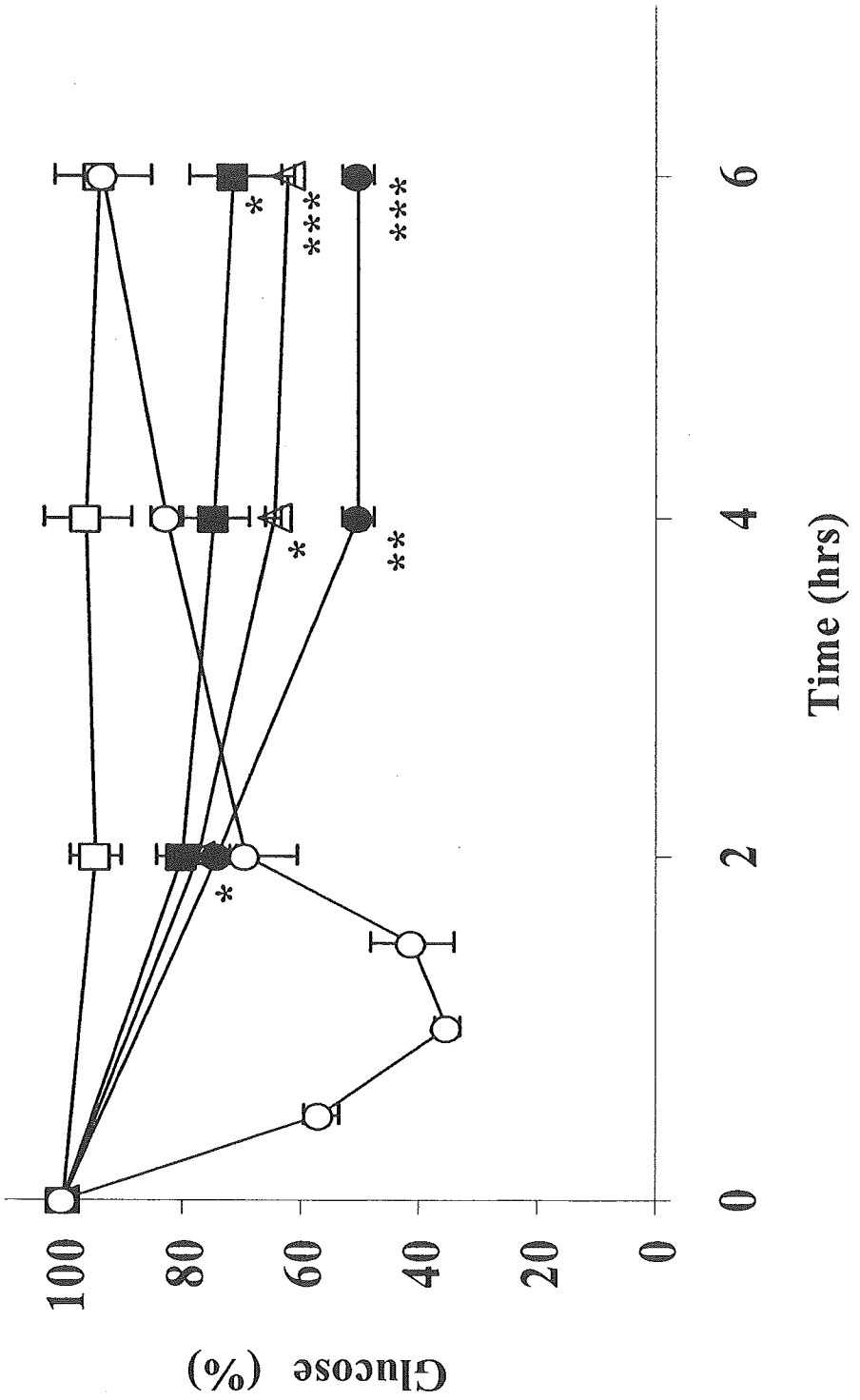

Available online at www.sciencedirect.com
SCIENCE DIRECT®
Journal of Controlled Release 110 (2006) 260 – 265
journal of controlled release
www.elsevier.com/locate/jconrel

Injectable porous hydroxyapatite microparticles as a new carrier for protein and lipophilic drugs

Yutaka Mizushima [a,*], Toshiyuki Ikoma [b], Jyunzo Tanaka [b], Keiko Hoshi [c], Tsutomu Ishihara [a], Yasuaki Ogawa [a], Akinori Ueno [a]

[a] *DDS Institute, Jikei University School of Medicine, 3-25-8, Nishi-Shimbashi, Minato, Tokyo 105-8461, Japan*
[b] *Biomaterials Center, National Institute for Materials Science, Namiki 1-1, Tsukuba, Ibaraki 305-0044, Japan*
[c] *Showa Pharmaceutical University, 3-3165, Higashi-tamagawagakuen, Machida, Tokyo 194-8543, Japan*

Received 16 August 2004; accepted 5 September 2005
Available online 28 November 2005

Abstract

Hydroxyapatite (Ca_{10} $(PO_4)_6(OH)_2$) is a biodegradable material that forms a major component of bones and teeth. We prepared injectable spherical porous hydroxyapatite microparticles (SP-HAp) as a drug carrier by the spray-drying method. We then examined the usefulness of SP-HAp as a carrier for drugs such as interferon alpha (IFNα), testosterone enanthate (TE), and cyclosporin A (CyA). SP-HAp had an average diameter of 5 μm and a porosity of approximately 58%. It could be injected subcutaneously through a 27-gauge needle. SP-HAp was observed to be biodegradable. The speed of degradation of SP-HAp could be regulated by altering the calcination temperature. IFNα was adsorbed well to SP-HAp particles, but INFα was released faster from the particles, than the particles could degrade in both in vitro and in vivo experiments. Addition of human serum albumin and zinc (reinforcement) to IFNα-adsorbed SP-HAp caused marked prolongation of release in vivo. The in vivo release of testosterone enanthate and CyA from SP-HAp preparation, which was easily injectable, was similarly prolonged to that from the oil preparation. In conclusion, the SP-HAp seems to be useful as a biodegradable and subcutaneously injectable drug carrier. It is suggested that the reinforcement of the SP-HAp is very effective on the sustained release of drugs.

Keywords: Hydroxyapatite; Drug delivery; Release kinetics; Degradation; Lipophilic drug

1. Introduction

Hydroxyapatite (Ca_{10} $(PO_4)_6(OH)_2$, HAp) is the main mineral component of bones and teeth, and it has been widely used in the orthopedic and dental fields as a paste, granules, or porous blocks for implants [1,2]. It is biodegradable, but the process is very slow. Hydroxyapatite is also utilized as an adsorbent during chromatography for purification and separation because of its excellent adsorption of many molecules [3–5]. Blocks of porous HAp and HAp ceramics have also been investigated for use in sustained-release drug delivery systems (DDS) for various therapeutic agents [6–10]. It has already been reported that implanted HAp preparations of antibiotics and anticancer drugs showed slow release in animals [8–10]. However, an injectable HAp preparation has not been reported previously. Moreover, there has been no report of injectable particles other than made of organic polymers, which can incorporate an adequate amount of drugs and can release them slowly.

In this study, we fabricated spherical porous HAp microparticles (SP-HAp) as an injectable carrier for drugs such as IFNα, TE, and CyA. Preparations of these drugs could be injected with a small-bore needle (27 gauge), which reduced pain on injection. We examined drug release from SP-HAp both in vitro and in vivo and also the preliminary reinforcement of this particle for the sustained release of drugs.

2. Materials and methods

2.1. Animals and drugs

For these studies, 36 ddY mice of either sex (8 weeks old) and 9 male Wistar rats (13 weeks old) were purchased from

* Corresponding author. Tel.: +81 3 5733 7390; fax: +81 3 5733 7397.
E-mail address: mizushima@ltt.co.jp (Y. Mizushima).

0168-3659/$ - see front matter © 2005 Elsevier B.V. All rights reserved.
doi:10.1016/j.jconrel.2005.09.051

Japan SLC (Hamamatsu, Japan). Experiments were conducted in accordance with the Guide for the Care and Use of Laboratory animals of Jikei University School of Medicine.

Interferon alpha (IFNα) was a kind gift from Sumitomo Pharmaceutical Co., Ltd. (Osaka, Japan). Testosterone enanthate (TE), cyclosporin A (CyA), and human serum albumin (HSA) were purchased from Wako Pure Chemical Industries (Osaka, Japan). An oil preparation of TE (Enarmon Depot) was obtained from Teikoku Hormone MFG Co., Ltd. (Tokyo, Japan). Mouse serum was purchased from Chemicon International, Inc. (Temecula, CA, USA).

2.2. Preparation of the spherical porous hydroxyapatite microparticles (SP-HAp)

CaO powder was obtained by heating 100 g of $CaCO_3$ powder (alkaline analytical grade, Wako Pure Chemical Industries, Osaka, Japan) at 1050 °C for 3 h, and was hydrated by addition of a one-third volume of distilled water to produce $Ca(OH)_2$. After adding 1000 ml of 0.6 M H_3PO_4 dropwise to 2000 ml of 0.5 M $Ca(OH)_2$ suspension at room temperature with vigorous stirring, the mixture was allowed to stand overnight. After adjusting the pH of the mixture to about 7.5, SP-HAp were fabricated by the spray-drying method. In brief, the suspension was atomized at a pressure of 1.5 MPa and a flow rate of 500 ml/h, while the inlet and outlet temperatures of the nozzle were adjusted to 180 °C and 80 °C, respectively. The product was lyophilized, and then heated at 180 °C, or calcined at 400 °C. SP-HAp that had been calcined at 400 °C for 0.5 h was used unless otherwise specified.

2.3. SP-HAp preparation of IFNα and lipophilic drugs

SP-HAp (200 mg) was added to 1 ml of the IFNα solution (80.4 μg) and then the resulting suspension was stirred for 10 min. After centrifugation (1700×*g* for 10 min), no IFNα was detected in the supernatant. In order to prolong the release of drugs from the SP-HAp preparations, the effect of adding human serum albumin (HSA) and zinc was examined. After the adsorption of IFNα to SP-HAp, 0.28 ml of a 35.73 mg/ml solution of HSA was added to the SP-HAp suspension. Then the dried precipitate was mixed thoroughly with 1 ml of 20 mM zinc acetate.

Fifty milligrams of SP-HAp calcined at 400 °C was mixed with 250 mg of testosterone enanthate dissolved in 200 μl of acetone. In the case of CyA, 10 mg of SP-HAp was mixed with 57 mg of CyA dissolved in 200 μl of ethanol. The suspensions were stirred vigorously to promote filling of the drugs (TE or CyA) into the pores of SP-HAp and then centrifugation was done at 1700×*g* for 5 min. After discarding the supernatant and then evaporating the excess solvent, the dried SP-HAp was used for in vivo studies.

2.4. Observation of SP-HAp by electron microscopy

SP-HAp was analyzed by powder X-ray diffractometry (XRD, PW1700, Philips Co., Germany) and Fourier-transformed infrared spectrometry (FT-IR, SPECTRUM-2000, Perkin-Elmer Inc., Welleslay, MA, USA). After the particles were coated with platinum, SP-HAp was observed by using a scanning electron microscope (SEM, JEOL-5600LV, Japan Electronics Co., Tokyo, Japan). The interior structure of the microparticles was observed by transmission electron microscopy (TEM, JEOL JEM-1010, Japan Electronics Co., Tokyo, Japan). Specimens 100 nm thick for TEM observation were prepared by embedding the microparticles in a light-cured resin, degassing under vacuum, and cutting on an ultramicrotome with a diamond knife. The surface area and total volume of the microparticles were determined by the Brunauer–Emmett–Teller method after being degassed at 200 °C for 2 h (SA-3100, Beckman-Coulter Inc., Fullerton, CA, USA). The particle size distribution was measured by the laser diffraction method (Salada-2100, Shimadzu Corp., Kyoto, Japan).

2.5. Biodegradability of SP-HAp in the subcutaneous tissue of rats

Three kinds of HAp preparation without a drug were used to assess the biodegradability of the microparticles in the subcutaneous tissue of rats. One was lyophilized HAp without calcination. After the spray-drying process, the other types of particles were heated at 180 °C or calcined at 400 °C, respectively. SP-HAp suspended in 5% mannitol (0.5 ml) was injected subcutaneously into the backs of Wistar rats and the animals were sacrificed on days 4, 7, 11, 14, 18, and 21. The amount of residual SP-HAp at the injection site was semi-quantitatively measured and a score was assigned as follows: 5 (no decrease), 4 (slight decrease), 3 (marked decrease), 2 (small amounts detected), 1 (particles hardly detected), and 0 (particles not detected). The average scores assigned by three independent observers were recorded.

2.6. Release of IFNα from SP-HAp in vitro and in vivo

One milliliter of an IFNα-containing SP-HAp suspension was added to 5 ml of phosphate-buffered saline containing 10% mouse serum (PBS-MS). With continuous shaking at 37 °C for 50 min to prevent precipitation of the particles, 500-μl aliquots of the suspension were taken at the 10-min intervals and the taken suspension was centrifuged (1700×*g* for 10 min at 4 °C) for the measurement of IFNα in the supernatant. In another experiment, the suspension was centrifuged and the supernatant was removed from the particles. Then 500 μl of supernatant was taken for IFNα analyses. Five milliliters of fresh PBS-MS (5 ml) was added to the particles for further incubation. The IFNα content was determined by using an ELISA kit (Biosource Inc., Sunnyvale, CA, USA).

In order to prevent the aggregation of HAp, 1 ml of 10% mannitol was added to 1 ml of SP-HAp suspension with or without HSA and zinc. IFNα (191 mg) dissolved in a solution (3.2 ml) of 0.75% HSA and 5% mannitol was also used. Then one of the two suspensions, SP-HAp preparation or the IFNα solution, was administered subcutaneously into the backs of male mice at a dose of 20 μg IFNα. Blood was collected from

the inferior ophthalmic vein at 0.5, 1, 2, 3, 4, 5, 6, and 10 days after injection and the plasma concentration of IFNα was measured with an ELISA kit as described above.

2.7. Release of TE or CyA from SP-HAp in vivo

SP-HAp filling TE or CyA was suspended in 0.3% carboxymethyl cellulose (CMC) solution. Then the SP-HAp suspension (23.8 mg in 250 μl per animal) or an oil preparation (29.9 mg in 250 μl per animal) of TE was administered subcutaneously into the backs of female mice. SP-HAp containing CyA (1.64 mg in 200 μl per animal) were injected also subcutaneously into the backs of male mice. Blood samples were taken from the inferior ophthalmic vein for determination of plasma TE and CyA concentrations with ELISA kits (Oxford Biomedical Research Inc., MI, USA).

3. Results

3.1. Characterization of the spherical porous hydroxyapatite microparticles (SP-HAp)

The crystal state of the HAp particles was investigated by XRD and FT-IR. SP-HAp calcined at 400 °C as well as lyophilized HAp was found to be homogenous. The XRD patterns showed that there were no crystals of calcium hydroxide ($Ca(OH)_2$), calcium oxide (CaO), tricalcium phosphate ($Ca_3(PO_4)_2$), or octacalcium phosphate. The FT-IR spectra revealed absorption bands assigned to the CO_3 group at 1458 and 1422 cm^{-1}, meaning that carbonate ions were substituted for phosphate in the crystal structure of HAp. The substituted carbonate ions were not decomposed by heating at 400 °C.

Fig. 1A shows an SEM photograph of SP-HAp: the microparticles are spherical with a rough surface because of nanopores. Fig. 1B shows a TEM photograph of SP-HAp, in which small (25 nm long and 5 nm wide) crystals of HAp are aggregated to form numerous interstitial spaces for adsorption of drugs. The porosity of SP-HAp was calculated from the theoretical density of HAp (3.156 g/cm^3). The surface area (per particle weight), the total volume (per particle weight), and the

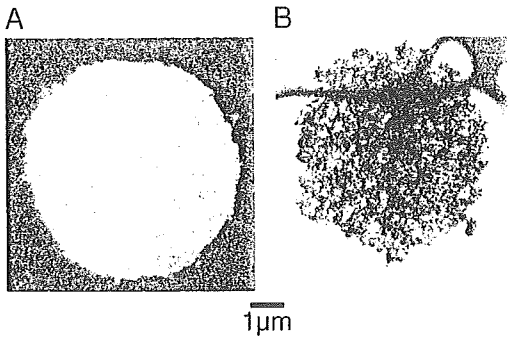

Fig. 1. SEM and TEM observation of spherical porous hydroxyapatite microparticles (SP-HAp). Panel A shows an SEM photograph of SP-HAP, which is approximately 5 μm in diameter. Panel B shows a TEM photograph or SP-HAp. Each crystallite in these microparticles prepared by spray drying measures 25 × 10 nm in size. Scale bar is shown for both panels.

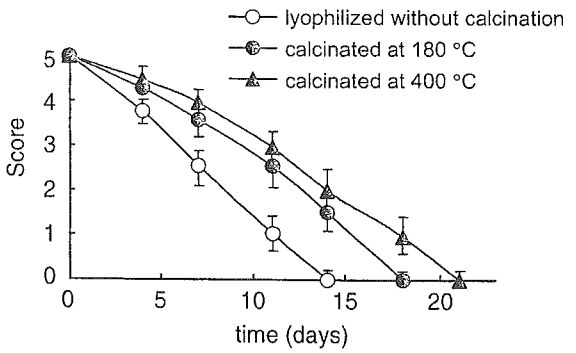

Fig. 2. Breakdown of SP-HAp after subcutaneous injection into rats. Three kinds of SP-HAp were prepared: (1) (open circles) lyophilization without calcination, (2) (closed circles) spray drying and calcination at a maximum of 180 °C, and (3) (closed triangles) spray drying and calcination at 400 °C. Disappearance of the microparticles was estimated by scoring as follows, 5 (no decrease), 4 (slight decrease), 3 (marked decrease), 2 (small amounts detected), 1 (particles hardly detected), and 0 (particles not detected). The symbols with vertical bars indicate the mean values and S.E.M.

porosity (as a percentage of the particle volume) were 87.9 m^2/g, 0.435 ml/g, and 57.8%, respectively, for lyophilized SP-HAp, while the values were 77.4 m^2/g, 0.413 ml/g, and 57.5% for SP-HAp calcined at 400 °C. Thus, the values of calcined SP-HAp were not significantly different from those of lyophilized SP-HAp. The average particle size was 5.8±1.6 μm for SP-HAp and 5.2±1.5 μm for SP-HAp calcined at 400 °C. The size distribution of either type of particle was in the range of 2–9 μm. Thus, calcination at 400 °C did not induce any dramatic changes of the surface area and particle size of SP-HAp.

3.2. Biodegradability of SP-HAp in rats

The biodegradability of SP-HAp containing no drugs was examined after subcutaneous injection into rats. Three kinds of the SP-HAp were prepared by lyophilization without calcinations (open circles) or by calcination at 180 °C (closed circles) and 400 °C (closed triangles). The residual amount of SP-HAp particles in the subcutaneous tissue was dependent on the calcination temperature, as shown in Fig. 2, because SP-HAp particles decreased in size or degraded slowly after calcination at 400 °C. Thus, the speed of the biodegradation of SP-HAp could be influenced by the fabrication method.

3.3. Release of IFNα from SP-HAp preparation in vitro

Fig. 3A shows the time course of the IFNα concentration in the supernatant without exchange of the incubation medium (PBS-MS). Release of IFNα was almost completed within 10 min and over 40% of the absorbed IFNα was released. After that, there was almost no further release unless the medium was changed.

The columns in Fig. 3B indicate the amount of IFNα released into the medium during each 10-min period when the medium was exchanged every 10 min. During the first period, about 40% of the absorbed IFNα was released into the medium. Subsequent release of IFNα was very small and

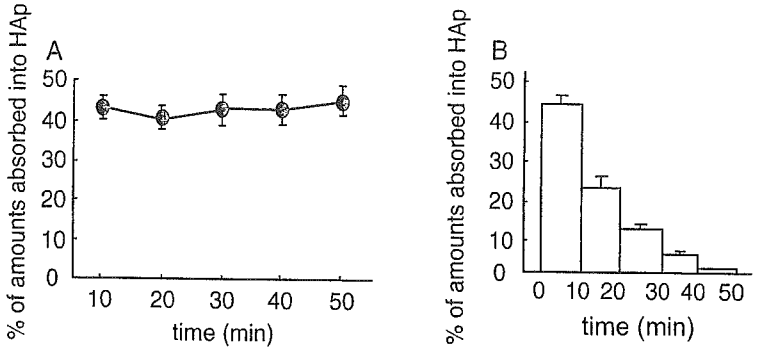

Fig. 3. In vitro release of IFNα from SP-HAp preparations into the PBS containing 10% mouse serum (PBS-MS). IFNα-containing SP-HAp was incubated in 5 ml of PBS-MS with shaking at 37 °C for 50 min. In panel A, 500-μl aliquots of the suspension were taken at the given times during incubation. In panel B, the incubation medium was exchanged every 10 min. Mean values of IFNα content with S.E.M. for three experiments are shown.

decreased over time. The value of the first 10-min period in Fig. 3B corresponds with it of the first 10 min in Fig. 3A. The accumulation of the amounts of IFNα released at 10-min intervals reached at least 90%.

3.4. Plasma IFNα concentration after subcutaneous injection of SP-HAp preparation

The plasma IFNα concentration was measured in mice after subcutaneous injection of the IFNα-containing SP-HAp preparation or IFNα solution (Fig. 4). When IFNα solution (open circles) was injected, the plasma IFNα concentration was initially very high and then decreased quickly. On day 3, no IFNα could be detected in the plasma. When the IFNα-containing SP-HAp preparation (closed triangles) was injected the initial burst was inhibited, but a similar plasma profile to the IFNα solution was observed after that. In contrast, the IFNα-containing SF-HAp preparation with HSA and zinc (closed circles in Fig. 4) showed sustained release of IFNα up to day 10.

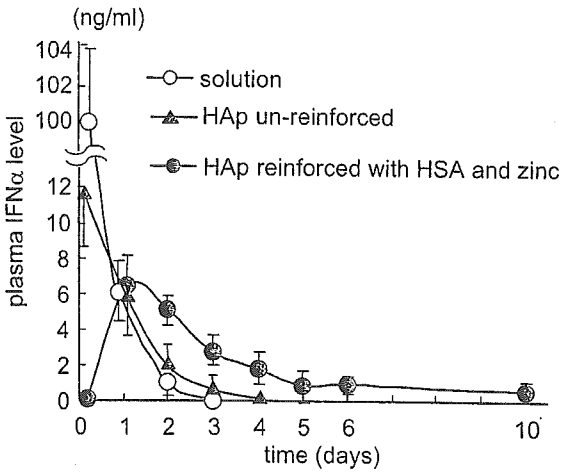

Fig. 4. The plasma concentration profile of IFNα after subcutaneous injection of SP-HAp preparation into mice. Animals received subcutaneous IFNα at a dose of 20 μg in each preparation. The currently available IFNα solution (open circles) and SP-HAp preparations with (closed circles) and without (closed triangles) reinforcement were tested. Mean values with S.E.M. for three experiments are shown.

3.5. Release of lipophilic drugs (TE or CyA) from SP-HAp preparation in vivo

Twenty two-gauge needle was required to subcutaneously inject the oil preparation of TE. However, preparations of SP-HAp containing TE or CyA could be injected easily through a much smaller-bore needle, such as a 27-gauge needle.

The plasma concentration profile of testosterone after subcutaneous injection of TE-containing SP-HAp (closed circles) is shown in Fig. 5A and is compared with that for the oil emulsion (open circles). The plasma concentration profile of testosterone was very similar for both preparations.

In Fig. 5B, the plasma concentration profile of CyA after subcutaneous injection of the CyA-containing SP-HAp preparation is shown. The peak plasma concentration of CyA was observed on day 1 after injection, while there was no longer any detectable CyA by day 3.

4. Discussion

It has been reported that HAp reversibly adsorbs many chemicals and proteins [3–5], suggesting that it would be a suitable carrier for drugs. In fact, a HAp carrier made by the spray-drying technique has already been used as a DDS [11], but there have been no reports about the use of HAp as injectable microparticles. In the present study, we fabricated spherical porous HAp microparticles (SP-HAp) by spray drying, and observation by electron microscopy showed that the HAp microparticles were composed of nanometer-sized homogeneous crystallites and were about 5 μm in average diameter. The SP-HAp prepared in this study could be injected subcutaneously as a suspension using a very narrow gauge needle, such as a 27-gauge needle. Our results also showed that SP-HAp had a very large surface area for the adsorption of drugs because the calculated porosity of the particles was nearly 60%. Kandari et al. reported good adsorption of immunoglobulin by various HAp particles [12]. In our experiment with IFNα (80 μg), no residual IFNα could be detected in the supernatant. This means that the amount of IFNα used was too small to fully saturate the microparticles. Although the maximum adsorption of IFNα by SP-HAp was not determined, it was demonstrated that the

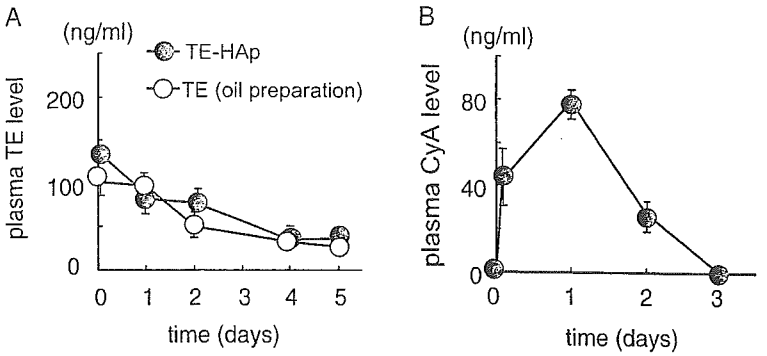

Fig. 5. The plasma concentration profiles of testosterone enanthate (TE) and cyclosporin A (CyA) after subcutaneous injection of SP-HAp preparations. In panel A, the results of TE as an SP-HAp preparation or an oil preparation (Enarmon Depot®) was shown. In panel B, the result of CyA as an SP-HAp preparation was shown. Each point with a vertical bar represents the mean value with S.E.M. for 3 experiments.

microparticles are able to adsorb a considerable amount of protein.

The biodegradability of three kinds of SP-HAp microparticles after subcutaneous injection was investigated in rats. Ito et al. also reported that HAp was biologically inert [13], so HAp microparticles should be safe for clinical use. Although there were differences in the persistence of the three types of microparticles, as shown in Fig. 2, all HAP particles mostly resolved after 21 days. Consequently, there is the potential to use these SP-HAp microparticles as a carrier scaffold for sustained-release of drug.

This study showed that the release of drugs was more rapid than the degradation of HAP microparticle. It has been reported that the physical properties of HAp can be altered by beating [14] and the temperature used in the process of HAp fabrication was reported to influence the release of protein drugs [15]. We used PBS containing 10% mouse serum in the present in vitro release experiments to obtain physiological conditions. From the data displayed in Fig. 3, it can be seen that the release of IFNα reached equilibrium within 10 min (Fig. 3A) and also that about 40–45% of the amount of IFNα remaining in the HAP microparticles was released each time the medium was changed at intervals of 10 min (Fig. 3B). Thus, release of IFNα from the microparticles in vitro was rather rapid and depended on factors such as the ionic strength and protein concentration of the incubation medium. These results suggest that the release of IFNα from SP-HAp will depend on the equilibrium concentration of the drug at the injection site. To use HAp as the carrier for a sustained-release drug preparation, it might be necessary to not only modify the manufacturing method to achieve slower release, but also to add other substances that delay release.

The current preparations of lipophilic drugs such as TE and CyA require a wide-bore needle (e.g. 22G) for injection. In contrast, TE- or CyA-containing SP-HAp preparations could be injected by using a small-bore needle (27G) and showed a similar pattern of drug release compared with the current slow-release oil preparation. Therefore, these microparticles may be useful for administration of lipophilic drugs.

Queiroz et al. used glass to delay drug release from porous HAp implants containing ampicillin [16]. There have been several other reports on the use of HAp combined with various substances, such as glass or polymers, to delay drug release [17–19]. In order to develop IFNα-containing SP-HAP as a slow-release preparation, the effect of HSA and zinc was examined in this study. These substances caused the prolongation of release in vivo (Fig. 4). Although further examination of the effects of other clinically available substances (reinforcement) will be required, the results of this study suggest the possibility of SP-HAp as an excellent drug carrier for sustained-release preparations.

5. Conclusion

This is the first report about the use of injectable spherical porous hydroxyapatite microparticles (SP-HAp) for drug delivery. In this study, we showed that SP-HAp preparations were biodegradable after subcutaneous injection and provided the sustained release of bioactive proteins and lipophilic drugs. It was also suggested that addition of certain substances (reinforcement) to SP-HAp was very effective for improving the sustained release of drugs.

Acknowledgements

This study was performed with Grants from the Ministry of Health, Labor and Welfare of Japan and the support of LTT Bio-Pharma Co., Ltd. We wish to thank Ms. A. Obata, Ms. E. Shimada, and Ms. H. Futagawa for their valuable technical assistance, as well as Ms. M. Hara for her assistance in preparing the manuscript.

References

[1] H. Oonishi, Orthopaedic applications of hydroxyapatite, Biomaterials 12 (1991) 171–178.
[2] D.G. Lange, D.C. Putter, Structure of the bone interface to dental implants in vivo, J. Oral Implantol. 19 (1993) 136–137.
[3] G. Bernardi, Chromatography of nucleic acids on hydroxyapatite columns, Methods Enzymol. 21 (1971) 95–139.
[4] M.J. Gorbunoff, Protein chromatography on hydroxyapatite columns, Methods Enzymol. 117 (1985) 370–380.
[5] S. Doonan, Chromatography on hydroxyapatite, Methods Mol. Biol. 244 (2004) 191–194.
[6] W. Paul, C.P. Sharma, Ceramic drug delivery: a perspective, J. Biomater. Appl. 17 (2003) 253–264.

[7] T. Matsumoto, M. Okazaki, M. Inoue, S. Yamaguchi, T. Kusunose, T. Toyonaga, Y. Hamada, J. Takahashi, Hydroxyapatite particles as a controlled release carrier of protein, Biomaterials 25 (2004) 3807–3812.
[8] A. Uchida, Y. Shinto, N. Araki, K. Ono, Slow release of anticancer drugs from porous calcium hydroxyapatite ceramic, J. Orthoptera Res. 10 (1992) 440–445.
[9] Y. Shinto, A. Uchida, F. Korkusuz, K. Araki, K. Ono, Calcium hydroxyapatite ceramic used as a delivery system for antibiotics, J. Bone Jt. Surg., Br. 74 (1992) 600–604.
[10] M. Itokazu, T. Sugiyama, T. Ohno, E. Wada, Y. Katagiri, Development of porous apatite ceramics for local delivery of chemotherapeutic agents, J. Biomed. Mater. Res. 39 (1998) 536–538.
[11] H.N. Pham, P. Luo, F. Genin, A.K. Dash, Synthesis and characterization of hydroxyapatite-ciprofloxacin delivery systems by precipitation and spray drying technique, AAPS PharmSciTech 3 (2002) E1.
[12] K. Kandari, K. Miyagawa, T. Ishikawa, Adsorption of gamma immuno globulin onto various synthetic calcium hydroxyapatite particles, J. Colloid Interface Sci. 273 (2004) 406–413.
[13] M. Ito, Y. Hidaka, M. Nakajima, H. Yagasaki, A.H. Kafrawy, Effect of hydroxyapatite content on physical properties and connective tissue reactions to a chitosan-hydroxyapatite composite membrane, J. Biomed. Mater. Res. 45 (1999) 204–208.
[14] S. Narayama, Kalkura, T.K. Anee, M. Ashok, C. Betzal, Investigation on synthesis and crystallization of hydroxyapatite at low temperature, Bio-Med. Mater. Eng. 14 (2004) 581–592.
[15] T. Matsumoto, M. Okazaki, M. Inoue, S. Yamaguchi, T. Kusunose, T. Toyonaga, Hydroxyapatite particles as a controlled release carrier of protein, Biomaterials 25 (2004) 3807–3812.
[16] A.C. Queiroz, S. Teixeira, J.D. Santos, F.J. Monteiro, Porous hydroxyapatite and glass reinforced hydroxyapatite for controlled release of sodium ampicillin, Key Eng. Mater. 254–256 (2004) 997–1000.
[17] Y.E. Greish, P.W. Brown, Characterization of bioactive glass-reinforced HAP-polymer composites, J. Biomed. Mater. Res. 52 (2000) 687–694.
[18] I. Balac, P.S. Uskokovic, R. Aleksic, D. Uskokovic, Predictive modeling of the mechanical properties of particulate hydroxyapatite reinforced polymer composites, J. Biomed. Res. 63 (2002) 753–799.
[19] C. Ritzoulis, N. Scoutaris, E. Demetriou, K. Papademetriou, S. Kokkou, S. Stavroulias, C. Panayiotou, Formation of hydroxyapatite/biopolymer biomaterials: I. Microporous composites from solidified emulsion, J. Biomed. Mater. Res. 71A (2004) 675–684.

CONTENTS

Cited in: BIOSIS/Biological Abstracts; CAB Abstracts; Chemical Abstracts Services; Current Contents (Life Sciences); EMBASE/Excerpta Medica; International Pharmaceutical Abstracts; PUBMED/MEDLINE/Index Medicus; Polymer Contents; Science Citation Index

(Contents continued on page 478)

0168-3659(20060110)110:2;1-0

05054

Available online at www.sciencedirect.com

SCIENCE DIRECT®

Journal of Controlled Release 105 (2005) 68–76

journal of controlled release

www.elsevier.com/locate/jconrel

Role of zinc in formulation of PLGA/PLA nanoparticles encapsulating betamethasone phosphate and its release profile

Tsutomu Ishihara[a,*], Nobuo Izumo[a], Megumu Higaki[b], Emi Shimada[a], Tomomi Hagi[a], Lisa Mine[b], Yasuaki Ogawa[b], Yutaka Mizushima[a,b]

[a]*DDS Institute, The Jikei University School of Medicine, 3-25-8 Nishi-shinbashi, Minato, Tokyo 105-8461, Japan*
[b]*Institute of Medical Science, St Marianna University School of Medicine, 2-16-1 Sugao, Miyamae, Kawasaki 216-8512, Japan*

Received 21 September 2004; accepted 28 February 2005

Abstract

The purpose of this study was to develop poly(D,L-lactic/glycolic acid) (PLGA) or poly(D,L-lactic acid) (PLA) nanoparticles of less than 200 nm in diameter that encapsulated water-soluble corticosteroid derivatives for sustained release and targeting to inflammatory sites. Nanoparticles were prepared with PLGA (or PLA), zinc, betamethasone phosphate and surfactant by an oil-in-water solvent diffusion method. With this method, the efficiency of encapsulating betamethasone phosphate in the nanoparticles and the particle size were significantly affected by various factors, such as the concentration of PLGA (or PLA) and the amount of zinc added. Nanoparticles ranging from 80 to 250 nm in diameter could be prepared, with a maximum betamethasone phosphate content of 8% (w/w). Betamethasone phosphate was gradually released from the nanoparticles in diluted serum, and the release rate depended on the glycolic/lactic acid ratio and on the molecular weight of PLGA or PLA. Betamethasone was gradually released over at least 8 days from murine macrophages that had internalized betamethasone phosphate-encapsulated nanoparticles in vitro, and the rate of release was slower than from nanoparticles prepared without zinc. These results suggest that zinc increases the efficiency of encapsulating betamethasone phosphate in nanoparticles and also promotes sustained release of betamethasone phosphate from the nanoparticles.

Keywords: PLGA; PLA; Nanoparticles; Zinc; Sustained release

1. Introduction

The biodistribution of systemically administered colloidal particles in the form of emulsions, liposomes and solid particles is markedly influenced by their diameter [1,2]. In our previous study, lipid nanospheres (lipid emulsions) with a diameter of approximately 200 nm accumulated in inflammatory sites after intravenous injection and were preferentially taken up by phagocytes such as macrophages and neutrophils [3,4]. Lipid nanospheres and liposomes, however, cannot retain bioactive molecules in the

* Corresponding author. Tel.: +81 3 3433 1111x2431; fax: +81 3 3438 2557.
E-mail address: ishihara@jikei.ac.jp (T. Ishihara).

0168-3659/$ - see front matter © 2005 Elsevier B.V. All rights reserved.
doi:10.1016/j.jconrel.2005.02.026

tissues for a long period. Thus, it is desirable to develop stable carriers with a diameter of 200 nm or less that have a sustained-release function for anti-inflammatory therapy by encapsulating bioactive molecules into solid particles consisting of biodegradable polymers such as poly(lactic/glycolic acid) (PLGA) and poly(lactic acid) (PLA).

Although many researchers have developed PLGA/PLA microparticles or nanoparticles encapsulating bioactive molecules including peptides, proteins and polynucleotides, few of these are used in clinical therapy. PLGA particles encapsulating a peptide prepared by the solvent evaporation method have been already used clinically, but the particles have a diameter in the micrometer size range and need to be administered subcutaneously [5,6]. In the case of PLGA/PLA nanoparticles with a suitable size for intravenous administration, major obstacles to clinical use include the complicated process of preparation and the low encapsulation efficiency of bioactive molecules. These obstacles have led researchers to develop simple methods for the preparation of nanoparticles. A solvent diffusion method in oil or in water possesses superior potential for the preparation of nanoparticles [7–9]. Hydrophilic and hydrophobic bioactive molecules were successfully incorporated into nanoparticles with a high efficiency by oil-in-oil and oil-in-water solvent diffusion methods, respectively [7–10].

In general, the efficiency of encapsulating bioactive molecules into PLGA/PLA microparticles/nanoparticles largely depends on the physical properties of the molecules. Chemical modifications of bioactive molecules such as esterification increase their encapsulation efficiency, but may decrease their bioactivity. On the other hand, there have been a number of reports that proteins and peptides stabilized in PLGA microparticles by the formation of a water-insoluble complex with metal ions such as zinc [11–15]. In addition, some researchers have reported that bivalent metal ions might slow the degradation of PLGA by increasing the microclimate pH toward neutral in PLGA microparticles [16,17] and films [18].

In the present study, a simple method was employed to prepare PLGA/PLA nanoparticles encapsulating water-soluble betamethasone phosphate (BP) in the presence of zinc. Investigations revealed that zinc played a significant role in the formulation of the nanoparticles and in modulation of the BP release profile.

2. Materials and methods

2.1. Materials

Poly(D,L-lactic/glycolic acid) (PLGA) with a lactic/glycolic acid ratio of 50/50 and poly(D,L-lactic acid) (PLA) were purchased from Wako Pure Chemicals Industries, Ltd. (Osaka, Japan). The molecular weight of the polymers was determined using gel permeation chromatography by Wako Pure Chemicals Industries. Betamethasone sodium phosphate, Pluronic F68 and egg yolk lecithin were purchased from Sigma Chemical Co. (St. Louis, MO, USA). Polyvinyl alcohol and Tween 20 were purchased from Wako Pure Chemicals Industries, Ltd. A time-resolved fluoroimmunoassay (TR-FIA) kit for betamethasone was supplied by Sionogi and Co., Ltd. (Osaka, Japan).

2.2. Interaction of metal ions with steroids

Hydrocortisone succinate aqueous solution neutralized by the addition of 1 M NaOH or betamethasone sodium phosphate aqueous solution (20 mM) was added to an equal volume of an aqueous solution containing metal ions at various concentrations. After 10 min, the mixture was centrifuged at 20,000×*g* for 10 min and the amount of steroids in the supernatant was determined by HPLC using a Symmentry 300™ C4 column (Waters Co., Massachusetts, USA).

2.3. Preparation of nanoparticles

Nanoparticles were prepared by an oil-in-water solvent diffusion method [7–9]. One milliliter of 0.5 M zinc acetate aqueous solution was added to 0.5 ml of an aqueous solution containing 4 mg of betamethasone sodium phosphate to form a betamethasone phosphate (BP)–zinc complex. After centrifugation at 20,000×*g* for 10 min, the resulting precipitated complex and 20 mg of PLGA (or PLA) were dissolved in acetone (0.5–1 ml). After addition of various volumes of 0.5 M zinc acetate aqueous solutions (0–

20 μmol), the solution was allowed for 1 h at room temperature. To 5 ml of an aqueous solution dissolved 25 mg of Pluronic F68, polyvinyl alcohol or Tween 20 or an aqueous suspension dispersed 25 mg of egg yolk lecithin, the acetone solution was added to obtain PLGA (or PLA) nanoparticles. Then, 1 ml of 0.5 M EDTA aqueous solution (pH 7.5) was added to the resulting nanoparticles suspension to chelate zinc in the BP–zinc complex. The nanoparticles were purified from unencapsulated BP by ultrafiltration (Centriprep YM-50, Amincon) and subsequent gel filtration (PD-10 column, Amasham Pharmacia). Finally, the nanoparticles suspension was freeze-dried in the presence of sucrose. Nanoparticles encapsulating rhodamine, a fluorescent dye, were prepared similarly. A mixture of 20 μl of 0.5 M zinc acetate aqueous solution and 0.7 ml of acetone dissolved 20 mg of PLGA (Mw 8000) and 1 mg of rhodamine was added to 5 ml of a 0.5% (w/v) egg yolk lecithin aqueous suspension. The resulting rhodamine-encapsulated nanoparticles were purified as mentioned above.

We also prepared nanoparticles by an oil-in-water solvent evaporation method. One milliliter of dichloromethane dissolved 30 mg of PLGA (or PLA), 3 mg of egg yolk lecithin and 1.5 mg of betamethasone dipropionate (BDP) was added dropwise to the 25 ml of distilled water. The mixture was sonicated for 10 min using a probe-type sonicator (output 80 W, UD-201, TOMY) and stirred for 2 h at room temperature using a magnetic stirrer. The resulting nanoparticles were purified as described above.

2.4. Characterization of nanoparticles

The particle size and distribution were determined by a dynamic light scattering method (FPAR-1000, Otsuka Electronics, Ltd., Osaka, Japan). The number average diameter calculated by Marquadt analysis is shown in this report. The nanoparticles were also observed using an Environmental Scanning Electron Microscope (ESEM-2700, Nikon Co., Tokyo, Japan). The BP or BDP content of the nanoparticles was determined as follows. The purified nanoparticles encapsulating BP or BDP were collected by centrifugation (20,000×g, 10 min) and washed once with distilled water by centrifugation. The precipitated nanoparticles were dissolved in acetonitrile, and the BP or BDP content was measured by HPLC using a Symmentry300™ C4 column. The precipitated nanoparticles were also freeze-dried and then weighed. The zinc content of the nanoparticles was determined using a sequential plasma spectrometer (ICPS-8000, Simadzu Co, Kyoto, Japan).

2.5. Release of betamethasone phosphate (BP) from nanoparticles

BP-encapsulated nanoparticles prepared with various polymers were dispersed in fetal bovine serum (FBS)/phosphate-buffered saline (PBS) (v/v, 1/1) at a nanoparticles concentration of 500 μg/ml. The suspension was incubated at 37 °C and the BP content of the nanoparticles was determined at specified times by HPLC as mentioned above.

2.6. Interaction of nanoparticles with macrophages in vitro

Inflammatory peritoneal macrophages were collected from the abdominal cavities of Balb/c mice that had been stimulated by intraperitoneal administration of 1.5 ml of 10% proteose peptone (Difco, Detroit, Mich.) [19]. The cells were harvested into each well of a 12-well cell culture plate at 6×10^5 cells/well and incubated overnight at 37 °C in 1 ml of Macrophage-SFM medium (Gibco™) containing antibiotics. Then, the medium was removed and the cells were incubated with 1 ml of fresh medium containing 25 μg of rhodamine-encapsulated nanoparticles. Two hours later, the cells were washed eight times with medium and were observed using a fluorescence microscope.

The release of betamethasone derivatives from murine macrophages was also evaluated. Murine macrophages were incubated with BP- (or BDP-) encapsulated nanoparticles and washed as described above. The cells were incubated at 37 °C and the medium was exchanged at specified intervals. The replaced medium was diluted and incubated with esterase (1.8 units/ml, from porcine liver, Sigma) in PBS or with alkaline phosphatase (2.7 units/ml, from calf intestine, Toyobo) in 1 M Tris–Cl buffer (pH 9.8, including 0.25 mM $MgCl_2$) for 1 h at 37 °C to obtain betamethasone prior to time-resolved fluoroimmunoassay. The total betamethasone content of the cells was also determined using a lysate prepared by repeated freezing/thawing of the cells.

3. Results and discussion

3.1. Interaction of metal ions with water-soluble steroids

Metal ions are essential to the body and are well known to form complexes with various molecules such as proteins, peptides and low molecular weight compounds. The water solubility of betamethasone phosphate (BP) and hydrocortisone succinate (HS) in the presence of various metal ions is shown in Fig. 1. A precipitate containing BP was formed in the presence of zinc or iron(II), indicating that BP changed to be hydrophobic. In contrast, magnesium did not induce precipitation of BP. Equivalent molar zinc and iron(II) could form a precipitate with mostly BP, suggesting these metal ions interacted with a phosphate group in BP by the ionic interaction. In the case of HS with a carboxyl group in the molecule, it was found that iron(II) caused slight precipitation of HS, but zinc did not. Therefore, the formation of water-insoluble complexes between metal ions and water-soluble steroids depended on the metal ion used and the functional groups in the steroid.

3.2. Preparation and characterization of nanoparticles

Preparation of nanoparticles by the solvent diffusion method is more likely to be applicable to mass production, compared with the solvent evaporation method or the spray drying method, because instruments such as a homogenizer are not required for the preparation. However, with the oil-in-oil solvent diffusion method, it is necessary to subsequently separate the nanoparticles from the oil by high-speed centrifugation [10]. Therefore, we tried to prepare the nanoparticles by an oil-in-water solvent diffusion method. Initially, the encapsulation of steroids in nanoparticles prepared in the presence or absence of metal ions was examined (Table 1). When nanoparticles were prepared in the absence of metal ions, hydrophobic betamethasone dipropionate (BDP) was encapsulated more effectively in the nanoparticles than hydrophilic BP or HS. On the other hand, addition of zinc significantly enhanced the efficiency of encapsulating BP in the nanoparticles, but not that of BDP. Iron(II) also enhanced the encapsulation of HS in nanoparticles, although the efficiency was lower than that of BP in the presence of zinc. The effective encapsulation of water-soluble steroids was achieved by an alteration in the hydrophobic nature of steroids through interaction with metal ions because the encapsulation efficiency corresponded with the formation of metal-steroid complexes. From the viewpoint of drug effect of steroids for anti-inflammatory therapy in clinical, it is presumed that nanoparticles with a ster-

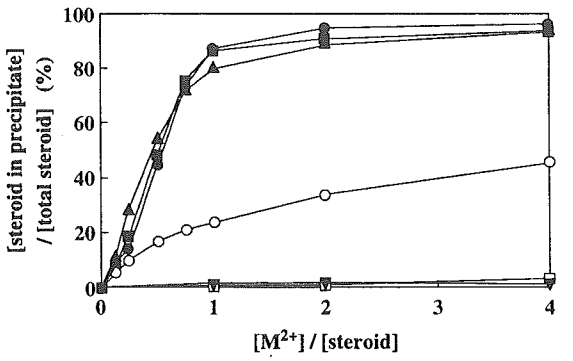

Fig. 1. Precipitation of water-soluble steroid derivatives in the presence of bivalent metal ions (M^{2+}). Betamethasone phosphate (BP) with (■) zinc chloride, (●) zinc acetate, (▲) iron(II) chloride or (▼) magnesium chloride. Hydrocortisone succinate (HS) with (○) iron(II) chloride or (□) zinc chloride.

Table 1
Preparation of nanoparticles encapsulating steroids by the solvent diffusion method

No.	Steroid	Metal ions	Steroid/nanoparticles (wt.%)	Diameter of nanoparticles (nm)
1	BP	None	0.02	90
2	BP	Zn^{2+}	5.02	138
3	HS	None	0.03	117
4	HS	Fe^{2+}	0.11	151
5	BDP	None	0.95	144
6	BDP	Zn^{2+}	1.10	136

BP: betamethasone phosphate, HS: hydrocortisone succinate, BDP: betamethasone dipropionate. The nanoparticles shown in nos. 1 and 3 were prepared by the addition of 300 μl of acetone with steroids and PLGA to 5 ml of water. The nanoparticles shown in nos. 2 and 4 were prepared by the addition of 500 μl of acetone containing the steroid-metal ions complex precipitate and PLGA to 5 ml of water as described in Section 2. The nanoparticles shown in nos. 5 and 6 were prepared by the addition of 500 μl of acetone dissolved PLGA and BDP in the absence or presence of 10 μmol zinc acetate to 5 ml of water. Twenty milligrams of PLGA (Mw 8000) and 4 mg of steroid were used for the preparation of all nanoparticles.

oid content of at least a few weight percent are desirable to be prepared. Thus, we estimated the encapsulation efficiency of BP in the nanoparticles prepared in the presence of zinc was enough.

Fig. 2 shows the diameter of nanoparticles obtained by varying the volume of solvent (acetone) and the amount of zinc acetate added, as well as the encapsulation efficiency of BP in these nanoparticles. The diameters of the nanoparticles and the encapsulation efficiency of BP increased with a decrease in the volume of acetone. Furthermore, the recovery efficiency of BP (weight ratio of total BP in nanoparticles to BP in feed) was low (below 30%). In the solvent diffusion method, it is considered that the nanoparticles are formed by diffusion of acetone in aqueous

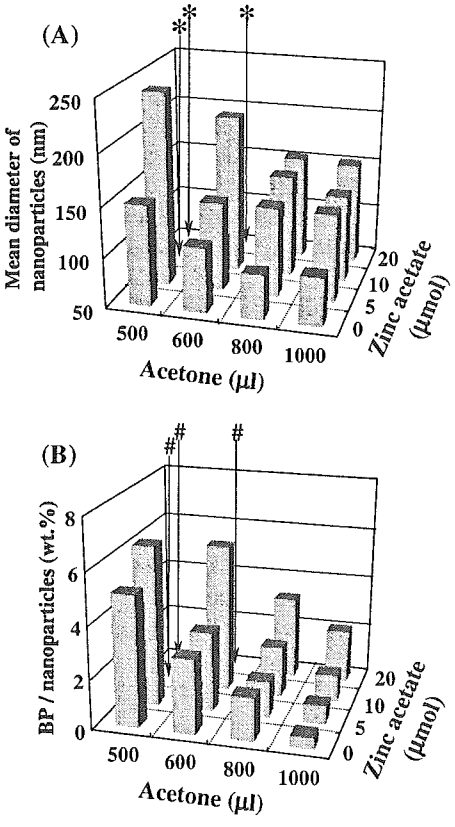

Fig. 2. Effect of the volume of acetone and amount of zinc acetate on the diameter of nanoparticles (A) and the encapsulation of BP in nanoparticles (B). Nanoparticles were prepared with 20 mg of PLGA (Mw 8000) and 4 mg of BP by the solvent diffusion method, as described in Section 2. *Aggregation of nanoparticles, #not determined.

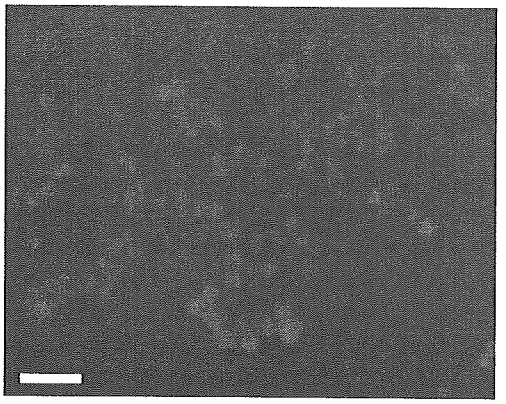

Fig. 3. SEM view of nanoparticles prepared by the solvent diffusion method. The nanoparticles were prepared with 20 mg of PLGA (Mw 8000), 4 mg of BP, 600 μl of acetone and 10 μmol zinc acetate. Bar=1 μm.

phase and subsequent condensation/solidification of PLGA [9]. Thus, our results strongly suggest that the nanoparticles were formed in the similar process. The shape of these nanoparticles was spherical and the size was considerably uniform, as shown in Fig. 3. It was also found that the surfactants, Pluronic F68, polyvinyl alcohol, Tween 20 and egg yolk lecithin in aqueous phase did not affect the encapsulation efficiency or the size of the nanoparticles (data not shown). Although equivalent zinc was enough to form a complex with BP as shown in Fig. 1, addition of more zinc increased the efficiency of encapsulating BP in the nanoparticles and the diameter (Fig. 2). This suggests another role of zinc in formulation of the nanoparticles.

The zinc content of nanoparticles with various amounts of BP was determined by sequential plasma spectrometry (Fig. 4). The zinc content increased along with the BP content of the nanoparticles, indicating the incorporation of BP as a complex with zinc. In nanoparticles prepared with zinc and PLGA (Mn 3400 and Mn 4700), the zinc content was 0.51 and 0.28 wt.% and the molar ratio of zinc to PLGA was calculated as 0.26 and 0.20, respectively. In addition, it was reported that zinc and cationic peptides interact with a carboxyl group at the terminal in PLGA molecules by the ionic interaction in microparticles [15,20]. As the molar ratio of zinc to PLGA in the nanoparticles formed from PLGA molecules with a different molecular weight was almost definite, zinc seemed to have a role in the formulation of nanopar-

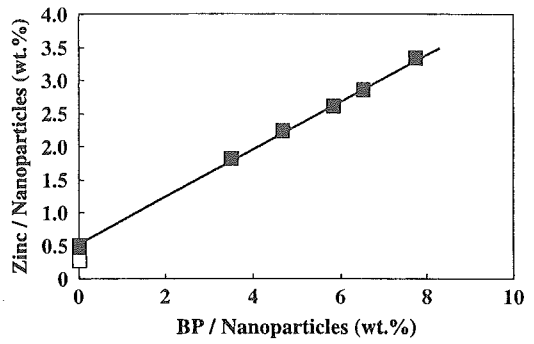

Fig. 4. Zinc and BP contents of nanoparticles. BP and zinc were determined by HPLC and sequential plasma spectrometry, respectively. Nanoparticles were prepared with (■) PLGA (Mn 3400, Mw 8000) or (□) PLGA (Mn 4700, Mw 13,000).

ticles by the ionic interaction in the same manner. Although it has been estimated that each zinc ion interacts with two PLGA molecules [15], the zinc content of the nanoparticles was not high enough for interaction with all of the carboxyl groups in the PLGA molecules, as described above. This might have been due to weak binding between zinc and PLGA.

The size of nanoparticles prepared with zinc was larger than that prepared without zinc (data not shown), indicating a change in more hydrophobic nature of PLGA by the neutralization of a carboxyl group in PLGA. The increase of the nanoparticles size by the interaction of zinc with PLGA might also enhance the encapsulation of BP in the nanoparticles. However, the size and the efficiency of encapsulating BDP in the nanoparticles were not significantly affected by addition of zinc (Table 1). The reason of the difference is likely to be due to the difference in the total amount of zinc added, but additional studies will be required to understand the role of zinc, PLGA and drugs in formulation of nanoparticles.

Table 2
Effect of the concentration of sucrose and the nanoparticles in the suspension on the dispersive stability of the nanoparticles after freeze-drying

Nanoparticles conc. (mg/ml)	Sucrose conc. (mg/ml)			
	0	20	50	100
5	*	145 nm	107 nm	92 nm
10	*	*	99 nm	97 nm
15	*	*	*	92 nm

The mean diameter of nanoparticles dispersed in water after freeze-drying is shown. The mean diameter of the nanoparticles before freeze-drying was 93 nm. *: not determined due to aggregate formation.

It is necessary to store nanoparticles in a freeze-dried form to prevent hydrolysis of PLGA/PLA. We examined the effect of additives on dispersive stability of the nanoparticles by analysis of the nanoparticles diameter after freeze-drying (Table 2). The nanoparticles were stably dispersed in water and their diameter was maintained when the suspension at a high concentration of sucrose and a low concentration of the nanoparticles was freeze-dried. This result indicates that sucrose at more than 5 times the weight of the nanoparticles should be added to the suspension to maintain the dispersive stability of freeze-dried nanoparticles (for example, the suspension consisting of 50 mg/ml sucrose and 10 mg/ml nanoparticles).

3.3. Profile of betamethasone phosphate release from nanoparticles

Fig. 5 shows the profile of BP release from the nanoparticles in diluted serum. Nanoparticles prepared by the current method released BP in a gradual manner. It was also found that nanoparticles formed from PLGA or from PLA with a low molecular weight tended to release BP faster than those with a high

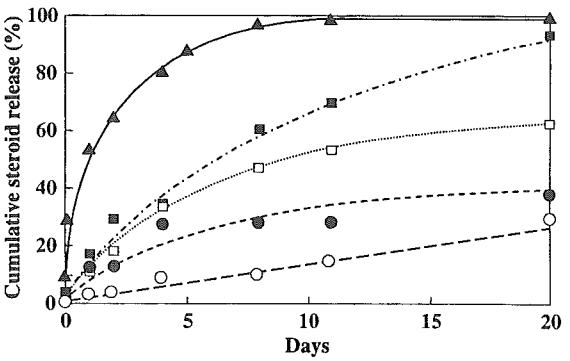

Fig. 5. Release profile of steroids from nanoparticles in FBS/PBS solution (50% v/v) at 37 °C. Nanoparticles encapsulating BP were prepared with different polymers (■: PLGA (Mw 8000), □: PLGA (Mw 13,000), ●: PLA (Mw 9000), ○: PLA (Mw 14,000)) by the solvent diffusion method. As a control, betamethasone dipropionate (BDP) release (▲) from nanoparticles prepared with PLA (Mw 14,000) by the solvent evaporation method is shown. Nanoparticles from 140 to 180 nm in diameter with a 4–5 wt.% content of steroids were used in this assay.